Malar stripe size and prominence in peregrine falcons vary positively with solar radiation: support for the solar glare hypothesis.

SUPPLEMENTARY MATERIAL

Vrettos, M., Reynolds, C. and Amar, A.

Author Contact Details

A. Amar:

Email: arjun.amar@uct.ac.za ; arjundevamar@gmail.com

Telephone: +27 (0)21 650 3304

C. Reynolds:

Email: chevonne.reynolds@gmail.com

Telephone: + 27 (0)11 717 6064

M. Vrettos:

Email: vrtmic003@myuct.ac.za

Telephone: 071 075 3443

Methods (Detail)

Sourcing photographs

We obtained photographs from two online citizen science repositories, the Macaulay Library at the Cornell Lab of Ornithology (https://www.macaulaylibrary.org/) and iNaturalist (https://www.inaturalist.org/). Within each photograph repository, we conducted 'country'-specific searches for photographs of peregrines. For North America, which covers a large geographic area and for which many photographs were available, we divided both the USA and Canada into their respective states or provinces and treated these as equivalent to separate countries. Likewise, offshore territories (e.g., Puerto Rico and the Virgin Islands) were treated as separate countries, as were England, Scotland, Wales, Northern Ireland and the Isle of Man. For iNaturalist, we used only 'Research Grade' observations. For the Macaulay Library searches, we ordered photographs from highest to lowest quality (based on user ratings) and downloaded the metadata for all photographs returned from each search, up to the website's limit of 10 000 photographs per query. This photograph metadata included the image URL, photographer's name, date, location, and GPS coordinates of the sighting. For the iNaturalist searches, which did not provide the ability to rank observations by quality, we filtered the metadata for all observations returned to include only the first 10 000 observations from each 'country'-specific search. We excluded all images tagged as juvenile or immature, or as species other than *Falco peregrinus*, including those tagged as Barbary Falcons (*Falco (peregrinus) pelegrinoides*/*babylonicus*), due to the unresolved and controversial taxonomic position of this taxon [1, 2].

We then downloaded JPEG versions of all images using the image URLs. We retained only photographs depicting adult birds, identified by the presence of horizontal barring (not vertical streaking or teardrop-shaped blotching) on the breast, yellow (not grey) cere, and slate-grey (not brown) dorsal feathers [1]. We also excluded photographs of misidentified birds (at the discretion of the observer, M. V.), as well as those identified as hybrids or captive by the photographer. To minimise pseudoreplication via repeated observations of the same individual, we excluded photographs taken at the same GPS location within a five-year time period as a previous photograph. However, we retained photographs from the same date and location if the birds could be readily distinguished as different individuals (e.g., based on plumage characters or rings). We also retained the few photographs that included multiple birds (N = 31).

For each ‘country’, we then selected a maximum of 50 random photographs for our analysis. This was done to ensure a sufficient sample to provide reliable estimates of malar stripe measurements for the ‘country’, while also ensuring that our dataset provided comprehensive coverage of the species’ geographic range and preventing any single region from dominating the sample. If any of the photographs returned from this random selection process were of insufficient quality for analysis, we removed these and repeated the selection process until we attained the maximum of 50 usable photographs per ‘country’, or until there were no more photographs available.

Scoring photographs

We quantified five aspects of the malar stripe: a) width, b) contiguity with the hood, c) prominence, and d) length (Figure S1, Figure S2), as well as e) an ‘elongation’ measure, which we calculated by dividing the length score by the width score. Scoring was performed on a per-individual rather than per-photograph basis, such that photographs that included two birds (N = 31) were treated as consisting of two observations. Thus, if a photograph depicted two birds, both birds were scored separately. Due to differences in scale, bird position and image resolution between photographs, we were unable to obtain quantitative morphometric measurements of the dimensions of the malar stripe for all individuals. Instead, all morphometric variables were defined relative to the width of the bird's eyeball in the photograph, measured from the medial to the lateral canthus of the eye (Figure S1). Malar stripe width was defined as the average thickness of the stripe, or the average horizontal distance from the proximal to the distal end of the dark plumage patch. Contiguity with the hood was defined as the extent of dark plumage in the area of the cheek between the malar stripe and the hood, or immediately posterior to the stripe (between the distal edge of the stripe and the distal point of the eye-ring). Malar stripe prominence was defined as the darkness or intensity of the stripe, measured by converting the image to greyscale and subjectively estimating the approximate tonal value of the stripe. Malar stripe length was defined as the vertical extent of the stripe, or the maximum vertical distance from the dorsal to the ventral end of the dark plumage patch. Malar stripe elongation was defined as the ratio of the vertical to the horizontal extent of the stripe, calculated as the ratio of the length score to the width score.

For each malar stripe variable analysed, M. V. constructed ten-point visual scales, based on qualitative visual assessment of variation in malar stripe characteristics observed in images of falcons (peregrines and closely related or visually similar species) sourced from Google Images (Figure S2). All individuals were scored visually according to these scales, with all scoring performed solely by M. V. to minimise observer effects. Scoring was also performed "blind", with all photographs pooled into a single folder and shuffled into a random order prior to scoring, and with the observer unaware of each photograph's geographic location during the scoring process. This was done to minimise the likelihood of systemic bias, either as a result of the observer knowing both the hypothesis under investigation and the geographical locations of the photographs, or due to photographs from the same geographic location being scored temporally adjacent to each other.

For each bird in each photograph, M. V. also recorded the approximate angle of the head (both horizontally, or in the plane perpendicular to the camera, and vertically, or in the plane parallel to the camera), as well as the approximate degree of shoulder hunching or neck compression leading to distortion of the cheek area (Figure S3). Head angle was assessed by assigning an approximate degree angle score to the bird's head based on its orientation towards the camera, measured in increments of 45°, according to a visual scale designed by M. V. (Figure S3). Neck compression or shoulder hunching was scored according to a four-point visual scale, which M. V. constructed based on the variation observed in photographs of peregrines sourced from Google Images (Figure S3). These scores were included as covariates in the GLS models to control for any variation in malar stripe scores due to differences in bird head position, since we suspected that the posture of the bird could influence visual assessment of malar stripe characteristics.

Validation of scores and shape analysis

As a complementary analysis to the subjective scores, and to validate the malar stripe measurements, we conducted a quantitative shape analysis on a representative subset of the data (N = 213 observations). To define this subset, we filtered the peregrine dataset to include only those individuals with a horizontal head angle score of 90°, a vertical head angle score of 0°, and a vertical compression score of 1 (see Figure S3 for reference). From these, we selected 213 observations that were both of high enough image quality for analysis, and that provided a representative subset of the larger dataset (in that they depicted birds of all malar stripe score categories in approximately the same proportions as in the larger dataset, and encompassed the full range of solar radiation values in the larger dataset). We then used the image processing software ImageJ [3] to quantify the shape of the malar stripe of each bird in this restricted sample. For each bird in each photograph, we first used the freehand selection tool to define a selection area corresponding to the entire dark plumage patch within the malar region (measured horizontally up to the distal corner of the eye-ring, and vertically up to the base of the eye-ring). We then converted these selections to binary image masks and standardized them to a width of 40px to control for differences in scale and image resolution between photographs. Using ImageJ, we then calculated the area, perimeter, circularity and roundness of the selection area within each binary image mask, along with the major and minor axis lengths and aspect ratio of the ellipse fitted to each selection (for more detailed definitions of these shape parameters and how they are calculated, see the ImageJ documentation [4]). All axis length, area and perimeter values were measured in pixels. Additionally, to validate our malar stripe prominence scores, we calculated the mean and median grey values of the pixels within the selection area in the original image. Grey values were assigned to pixels based on their luminosity or brightness, such that darker pixels had lower values.

For the 213 observations for which we had quantitative measurements available, we then calculated Pearson’s correlation coefficients between the quantitative measurements and our original subjective scores. We were unable to reliably assess the relationships between the climate variables and the quantitative measurements due to the restricted sample size.

Results: Validation of Scores and Shape Analysis (Detail)

Malar stripe width, contiguity and length scores were all significantly ($p < 0.001$) positively correlated with the area in pixels of the malar stripe, with correlation coefficients between 0.40 and 0.50 (Figure S5). Malar stripe elongation scores were likewise negatively correlated with the area in pixels of the malar stripe (Figure S5). In contrast, the perimeter of the malar stripe was positively related to length and elongation (Figure S5). The circularity and roundness of the malar stripe selections were positively related to both the width and contiguity scores, but were negatively related to elongation and unrelated to length (Figure S5). The major (vertical) axis lengths of the ellipses fitted to the selections correlated positively with length scores, while the minor (horizontal) axis lengths exhibited strong positive correlations with width and contiguity, a weaker positive correlation with length, and a negative correlation with elongation (Figure S5). The aspect ratios of the fitted ellipses likewise correlated negatively with width and contiguity and positively with elongation, but were unrelated to length (Figure S5). Larger malar stripes thus tended to receive higher width, contiguity and length scores and lower elongation scores, while those that received higher width and contiguity scores also tended to be rounder and more regular (less elongated) in shape. Relatively shorter and wider malar stripes thus tended to be larger in terms of total area than relatively longer and thinner malar stripes. Malar stripe prominence scores were, unsurprisingly, unrelated to any of the quantitative shape measurements, but were significantly ($p < 0.001$) negatively correlated with both the mean and median pixel grey values of the malar stripe, indicating that darker malar stripes received higher prominence scores (Figure S5). We were thus able to conclude that our subjective scores approximately captured real variation in peregrine malar stripe characteristics.

Table S1. Sample sizes of usable peregrine photographs, and total numbers of individual birds represented in these photographs, obtained from the Macaulay Library and iNaturalist for each 'country' represented in the dataset, along with their mean malar stripe scores and average annual solar radiation (W/m^2). All scoring and analysis was performed on a per-individual bird rather than per-photograph basis, such that photographs that included two birds (N = 31) were counted as two observations.

'Country'	Individuals	Photographs	Malar Stripe Width (Mean)	Malar Stripe Contiguity (Mean)	Malar Stripe Prominence (Mean)	Malar Stripe Length (Mean)	Malar Stripe Elongation (Mean)	Average Annual Solar Radiation (W/m^2)
Alabama	9	9	6.22	4	7.89	7.78	1.31	1899.25
Alaska	24	23	6.13	3.88	8.29	8.38	1.39	937.922
Alberta	18	18	6.22	3.83	8.33	8.67	1.44	1484.92
Algeria	14	13	5.5	3.57	7.5	7.71	1.44	2018.96
Angola	2	2	6	5	8.5	9	1.54	1752.82
Argentina	40	40	7.5	5.45	8.33	8.28	1.18	1863.59
Arizona	45	44	7.4	5.36	7.93	8.47	1.22	2249.12
Arkansas	5	5	7.8	4.4	9.2	8.8	1.15	1782.72
Armenia	1	1	6	3	10	9	1.5	1806.48
Australia	48	47	9.27	9.1	9.46	8.35	0.94	2010.81
Austria	1	1	7	4	8	8	1.14	1351.85
Bahamas	8	8	6.5	5.13	8.63	7.38	1.2	2129.46
Bangladesh	3	3	5.33	3.67	7.67	7.67	1.46	2048.54
Belgium	1	1	10	10	10	8	0.8	1197.12
Belize	11	11	6.45	3.45	8.64	9	1.47	2115.04
Bhutan	2	2	7	7.5	9	7.5	1.06	1888.83
Brazil	15	15	6.07	3.2	8.53	7.53	1.27	1688.17
British Columbia	45	44	7.16	4.91	8.33	8.2	1.18	1360.71
Brunei	1	1	10	10	10	9	0.9	2080.63
California	44	44	7.43	5.48	8.23	8.16	1.14	1973.62
Cambodia	1	1	6	4	8	8	1.33	2227.45
Cayman Islands	4	4	7.25	4.25	9	7.75	1.07	2275.01
Chile	20	20	6.75	4.45	8.35	7.8	1.26	1821.72
China	7	7	6.14	4.43	8.71	8.86	1.79	1714.2
Colombia	5	5	5	2.8	8.4	9.2	1.88	1801.47
Colorado	46	46	6.96	4.63	8.67	8.46	1.27	1935.37
Connecticut	32	29	6.91	4.97	8.52	8.39	1.25	1558.42
Costa Rica	23	23	6.74	4.78	8.7	8.13	1.26	2296.49
Croatia	1	1	4	4	10	8	2	1514.01

Cuba	2	2	7	2.5	9.5	8	1.19	2255.88
Czech Republic	2	2	6.5	4	7	9.5	1.46	1264.88
Delaware	9	9	6.33	3.67	8.89	8.67	1.48	1641
Denmark	1	1	7	7	7	3	0.43	1137.81
District of Columbia	8	8	6.63	4.63	7.63	8	1.24	1639.33
Dominica	1	1	4	2	7	9	2.25	2257.85
Dominican Republic	1	1	7	4	10	6	0.86	2196.37
Democratic Republic of the Congo	1	1	6	5	8	6	1	1960.09
Ecuador	7	7	6.43	5.29	8.86	7.71	1.25	1614.07
El Salvador	13	13	6.54	4.54	8.38	8.69	1.43	2240.72
England	42	42	6.21	5.43	8.29	8.52	1.43	1145.05
Ethiopia	4	1	6.75	5.5	9	8.5	1.28	2326.91
Falkland Islands (Malvinas)	1	1	10	10	9	10	1	1258.14
Finland	1	1	6	5	7	10	1.67	971.522
Florida	44	44	6.3	3.66	8.52	8.64	1.42	2028.02
France	15	15	6.53	4.8	8.27	7.87	1.25	1551.99
Georgia (USA)	13	13	7.08	5.23	8.15	8.31	1.21	1814.67
Germany	7	7	6.57	3.43	7.57	7.29	1.18	1235.66
Greece	1	1	6	3	10	8	1.33	1702.01
Greenland	1	1	6	3	10	10	1.67	987.786
Guatemala	4	4	7	6.5	9.25	9.75	1.43	2149.42
Guyana	2	2	7	5	8.5	8	1.17	2139.22
Haiti	2	2	7.5	5	8.5	9.5	1.27	2100.62
Honduras	13	13	6.46	4.92	8.92	8.08	1.43	2311.33
Hong Kong	5	5	7.8	6.4	9	8.4	1.14	1645.25
Idaho	12	12	7	5	7.67	8.17	1.21	1724.73
Illinois	41	41	6.71	5.02	7.71	7.85	1.21	1588.55
India	36	36	5.75	3.81	8.39	8.28	1.54	2216.68
Indiana	21	20	6.05	4.48	7.9	8.52	1.48	1603.98
Indonesia	5	5	8	6.4	9	8.8	1.14	2069.4
Iowa	12	12	5.5	3.92	8.67	7.67	1.46	1624.61
Iran	2	2	5	2.5	7	7.5	1.5	2323.87
(Republic of) Ireland	2	2	6.5	5.5	8	6.5	1.02	1112.68
Israel	5	5	5.2	3.2	7.2	8.6	1.93	2261.58
Italy	16	16	5.81	3.69	8.94	8.19	1.44	1633.73
Jamaica	1	1	6	3	10	8	1.33	2171.22
Japan	11	11	5.36	4	8.09	8.91	1.72	1594.35

Kansas	7	7	6.43	4.71	8.57	8.86	1.45	1819.62
Kentucky	12	11	6.58	4.58	8.17	8.5	1.44	1683.91
Kenya	1	1	3	4	8	9	3	1983.83
Latvia	1	1	5	2	8	10	2	1166.25
Lebanon	1	1	6	3	10	10	1.67	2046.97
Louisiana	21	21	7.24	5.38	8.48	8.19	1.18	1880.1
Madagascar	3	3	5.67	4.33	10	9	1.61	2394.24
Maine	38	38	6.61	4.47	7.84	8.32	1.3	1491.37
Malaysia	6	6	6.5	4	9	7.83	1.36	1753.1
Manitoba	5	5	5.4	3.4	9.2	8.4	1.58	1373.9
Maryland	38	36	6.89	4.71	8.08	8.29	1.24	1635.6
Massachusetts	46	44	6.61	4.3	8	7.93	1.23	1528.6
Mexico	47	46	7.3	5.64	8.77	8.62	1.21	2109.29
Michigan	41	39	6.68	4.54	8.02	8.24	1.26	1508.59
Minnesota	32	32	6.44	4.41	8.06	8	1.27	1493.83
Mississippi	2	2	6	4	7.5	8.5	1.5	1888.37
Missouri	10	10	6.2	3.5	8.7	7.4	1.2	1707.24
Mongolia	1	1	4	4	9	8	2	1926.65
Montana	20	20	7.05	5.55	8.5	8.15	1.2	1611.63
Morocco	5	5	5.4	4.2	8	8.2	1.56	2124.35
Myanmar	1	1	6	3	7	7	1.17	2108.03
Nebraska	6	6	6.67	3.83	7.5	8.33	1.3	1724.97
Nepal	1	1	5	2	6	7	1.4	2106.26
Netherlands	2	2	6	4	7.5	7.5	1.27	1150.75
Nevada	17	16	7.24	5.82	8.12	7.82	1.18	2150.16
New Brunswick	9	9	5.67	3.22	8.67	7.33	1.46	1443.75
New Caledonia	1	1	6	8	10	8	1.33	2206.38
New Hampshire	17	17	6.88	4.53	7.88	7.29	1.11	1509.63
New Jersey	39	38	6.69	4.9	8.26	7.77	1.2	1624.41
New Mexico	38	38	7.16	4.42	8.53	8.34	1.2	2201.24
New York	42	42	6.4	4	8.14	7.64	1.25	1525.48
Newfoundland and Labrador	6	6	6.5	3.5	8.67	8.5	1.34	1282.3
Nicaragua	8	8	7	5.75	9	8.63	1.28	2375.14
North Carolina	23	23	6.52	4.35	8.3	8.17	1.28	1773.79
North Dakota	6	6	7	3.67	8	7.17	1.05	1478.47
Northern Ireland	3	3	5.33	5.33	9	8.33	1.56	1031.95
Northwest Territories	2	2	5.5	2	9.5	10	1.83	1203.28
Norway	1	1	8	3	7	7	0.88	1055.09
Nova Scotia	29	28	6.17	4.07	8.24	8.1	1.36	1444.6
Nunavut	1	1	6	4	10	8	1.33	1196.88

Ohio	39	38	6.74	4.54	8.46	7.9	1.2	1541.87
Oklahoma	7	7	7	5.43	9.43	9.43	1.36	1978.63
Oman	1	1	4	1	9	7	1.75	2458.19
Ontario	43	42	6.44	3.74	8.14	8.33	1.33	1491.31
Oregon	42	42	7.07	5	8.17	8.38	1.22	1514.28
Pakistan	2	2	4	1.5	8.5	9	2.4	1734.24
Panama	13	13	6.15	3.46	8.69	9	1.53	2210.59
Paraguay	1	1	5	2	10	9	1.8	1912.17
Pennsylvania	36	34	6.56	4.61	8.06	7.64	1.2	1564.92
Peru	28	28	6.39	3.75	8.61	7.96	1.31	1809.28
Philippines	4	4	5	3.5	7.25	8	1.67	1849.54
Portugal	40	39	5.75	4.23	7.98	8	1.49	1934.41
Prince Edward Island	1	1	4	4	9	7	1.75	1419.62
Puerto Rico	11	11	6.36	4.55	8.45	8.73	1.41	2160.46
Quebec	40	39	6.53	4.6	7.93	8.1	1.34	1452.94
Rhode Island	9	9	5.67	3.89	8.33	7.89	1.44	1557.51
Romania	1	1	6	4	6	9	1.5	1612.28
Russia	14	14	6.14	4.14	9.07	8.29	1.4	1334.23
Saskatchewan	10	10	7.2	4.9	8.5	8.8	1.23	1479.91
Scotland	2	2	5	3.5	9	6.5	1.38	986.653
Seychelles	1	1	6	4	10	10	1.67	2541.58
Singapore	3	3	6.67	6	9.33	9.33	1.53	1777.07
South Africa	15	15	6	3.93	8.67	8	1.41	2098.2
South Carolina	9	9	6.33	4.11	8.56	8.11	1.35	1862.31
South Dakota	2	2	6.5	2.5	8.5	9.5	1.56	1607.06
South Korea	2	2	5	5	9	9.5	1.9	1529.67
Spain	39	39	5.92	4.56	8.23	7.77	1.38	1794.85
Sri Lanka	2	2	7.5	6	9.5	7.5	1.15	2320.38
Sweden	5	5	4.8	3	7.8	7.8	1.62	1143.84
Switzerland	2	2	6	4.5	7	9.5	1.64	1453.1
Taiwan	29	28	6.21	4.41	8.72	8.28	1.37	1792.73
Tanzania	2	2	5.5	3.5	9.5	6.5	1.2	1960.17
Tennessee	7	7	6.71	4.14	8.86	8.71	1.41	1747.43
Texas	41	41	6.66	4.32	8.32	8.34	1.3	1974.71
Thailand	13	13	6.31	4.38	8.15	7.38	1.24	2169.67
Trinidad and Tobago	9	9	6	2.89	8.33	7.78	1.32	2115.31
Turkey	9	9	5.67	3.89	7.78	7.89	1.47	1923.54
Ukraine	1	1	9	5	9	8	0.89	1389.65
United Arab Emirates	1	1	5	4	6	8	1.6	2502.87

Uruguay	5	5	6	3.4	7.2	7.8	1.28	1921.53
Utah	37	37	6.97	4.54	8.59	8.41	1.26	1949.83
Venezuela	4	4	6.5	4.25	8.5	7.75	1.26	2174.61
Vermont	44	43	6.68	4.39	8.61	8.16	1.26	1472.85
Vietnam	3	3	6.33	3.33	8.33	8	1.31	2019.21
Virginia	41	40	6.22	4	8.1	7.78	1.29	1690.08
Wales	2	2	5.5	5.5	8	9.5	1.73	1110.54
Washington	39	39	6.92	5.23	8.26	7.85	1.2	1395.91
West Virginia	3	3	7	5.67	7.67	7	1.06	1576.12
Western Sahara	1	1	6	2	10	8	1.33	2357.38
Wisconsin	39	39	6.51	4.44	8.03	7.72	1.2	1520.26
Wyoming	5	5	6.6	4.6	8.4	8.4	1.38	1724.91
Yukon Territory	5	5	6.4	4	9	7.8	1.23	940.49
Zambia	3	3	6.33	6	9.67	8	1.3	2071.85
Zimbabwe	1	1	6	3	10	7	1.17	2275.52
Total	**2197**	**2166**						

Table S2. Model-averaged parameter estimates for the effects of the three climate predictor variables (average annual solar radiation (W/m^2), average annual rainfall (mm), and average minimum daily temperature (°C)) on each of the five malar stripe variables, with associated standard errors and 95% confidence intervals. Model-averaged parameter estimates were calculated with candidate models weighted by their AICc values. Predictor variables whose 95% confidence intervals overlap zero are considered to have no effect on the response.

Model	**Estimate**	**SE**	**95% CI LL**	**95% CI UL**
Width				
Solar Radiation	0.28	0.04	0.19	0.37
Rainfall	-0.03	0.04	-0.11	0.05
Minimum Temperature	-0.24	0.05	-0.34	-0.15
Contiguity				
Solar Radiation	0.14	0.06	0.02	0.25
Rainfall	-0.18	0.05	-0.28	-0.08
Minimum Temperature	-0.01	0.09	-0.20	0.17
Prominence				
Solar Radiation	0.11	0.04	0.04	0.18
Rainfall	0.03	0.03	-0.03	0.10
Minimum Temperature	-0.04	0.05	-0.14	0.05
Length				
Solar Radiation	0.03	0.04	-0.04	0.11
Rainfall	0.03	0.03	-0.04	0.09
Minimum Temperature	-0.05	0.04	-0.13	0.03
Elongation (Length/Width)				
Solar Radiation	-0.04	0.01	-0.06	-0.02
Rainfall	0.01	0.01	-0.01	0.03
Minimum Temperature	0.04	0.01	0.02	0.07

Table S3. Model-averaged parameter estimates for the effects of the three climate predictor variables (average annual solar radiation (W/m^2), average annual rainfall (mm), and average minimum daily temperature (°C)) on each of the five malar stripe variables with the analysis filtered to include only resident and breeding birds (N = 891), with associated standard errors and 95% confidence intervals. Model-averaged parameter estimates were calculated with candidate models weighted by their AICc values. Predictor variables whose 95% confidence intervals overlap zero are considered to have no effect on the response.

Model	**Estimate**	**SE**	**95% CI LL**	**95% CI UL**
Width				
Solar Radiation	0.28	0.07	0.14	0.41
Rainfall	0.01	0.07	-0.13	0.16
Minimum Temperature	-0.17	0.07	-0.30	-0.03
Contiguity				
Solar Radiation	0.26	0.09	0.08	0.43
Rainfall	-0.13	0.11	-0.34	0.08
Minimum Temperature	0.14	0.14	-0.14	0.42
Prominence				
Solar Radiation	0.11	0.06	0.00	0.22
Rainfall	-0.01	0.06	-0.12	0.10
Minimum Temperature	-0.09	0.06	-0.21	0.03
Length				
Solar Radiation	0.05	0.05	-0.06	0.16
Rainfall	0.00	0.05	-0.10	0.11
Minimum Temperature	-0.07	0.05	-0.18	0.03
Elongation (Length/Width)				
Solar Radiation	-0.04	0.02	-0.07	-0.01
Rainfall	0.00	0.02	-0.03	0.03
Minimum Temperature	0.03	0.02	0.00	0.06

Table S4. Model-averaged parameter estimates for the effects of the three climate predictor variables (average annual solar radiation (W/m^2), average annual rainfall (mm), and average minimum daily temperature (°C)) on each of the five malar stripe variables with the analysis filtered to exclude the USA and Canada (N = 764), with associated standard errors and 95% confidence intervals. Model-averaged parameter estimates were calculated with candidate models weighted by their AICc values. Predictor variables whose 95% confidence intervals overlap zero are considered to have no effect on the response.

Model	Estimate	SE	95% CI LL	95% CI UL
Width				
Solar Radiation	0.30	0.07	0.15	0.44
Rainfall	0.01	0.06	-0.10	0.12
Minimum Temperature	-0.33	0.09	-0.51	-0.15
Contiguity				
Solar Radiation	0.30	0.11	0.09	0.51
Rainfall	-0.06	0.09	-0.23	0.11
Minimum Temperature	-0.51	0.15	-0.80	-0.22
Prominence				
Solar Radiation	0.10	0.05	0.00	0.21
Rainfall	0.05	0.04	-0.04	0.13
Minimum Temperature	-0.07	0.09	-0.25	0.11
Length				
Solar Radiation	0.00	0.05	-0.09	0.10
Rainfall	0.07	0.04	0.00	0.14
Minimum Temperature	-0.06	0.07	-0.19	0.07
Elongation (Length/Width)				
Solar Radiation	-0.04	0.02	-0.08	0.00
Rainfall	0.02	0.01	0.00	0.05
Minimum Temperature	0.04	0.03	-0.01	0.01

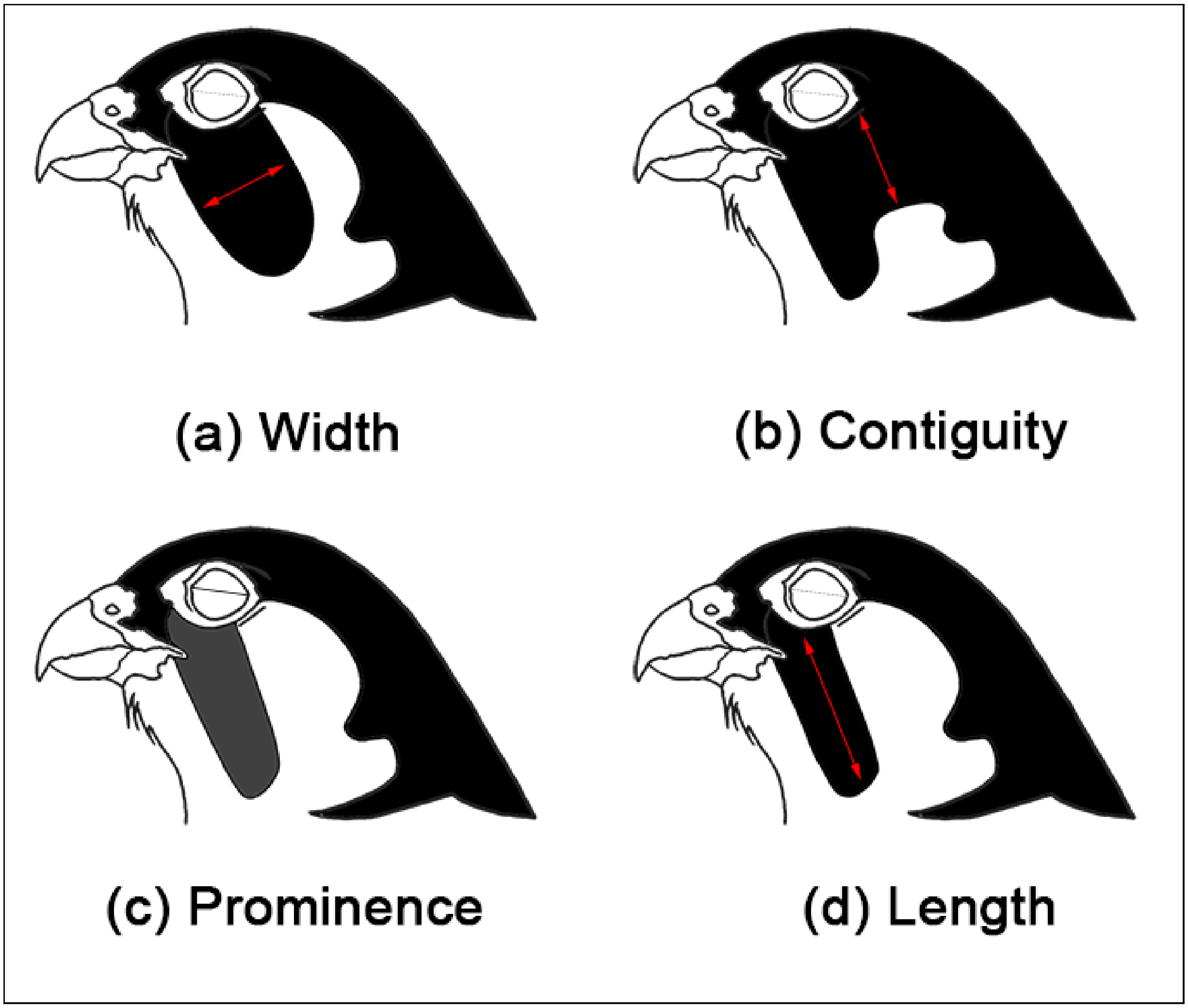

Figure S1. Diagram illustrating four of the five aspects of the malar stripe we quantified in this study, namely **(a)** malar stripe width, **(b)** contiguity between the malar stripe and the hood, **(c)** malar stripe prominence and **(d)** malar stripe length, as well as our reference measurement (the width of the eyeball). Elongation scores were calculated by dividing the length score by the width score for each observation. A more detailed guide to our visual scoring of malar stripe characteristics is provided in Figure S2.

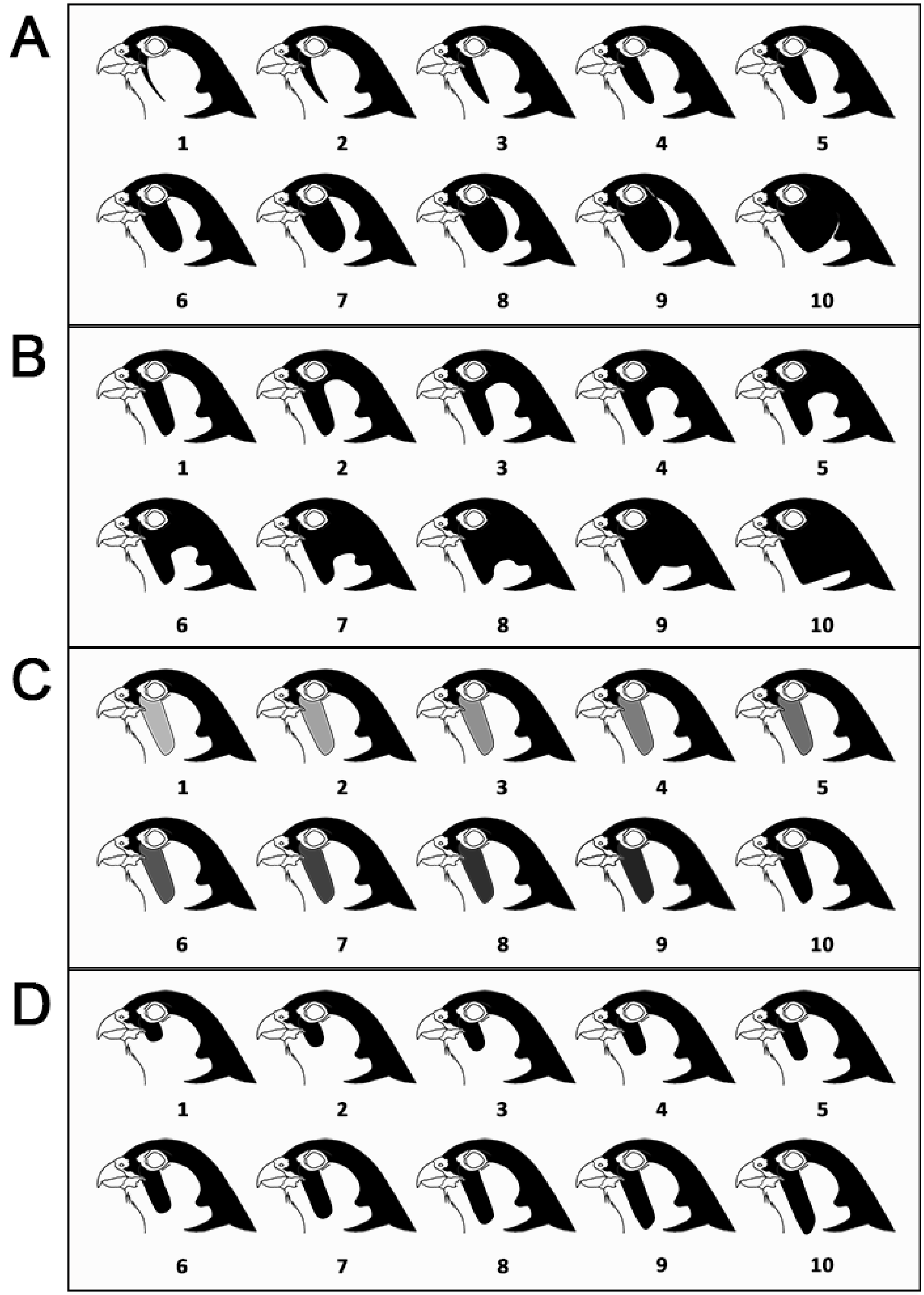

Figure S2. Diagram illustrating the ten-point visual scales used to quantify variation in **(A)** malar stripe width, **(B)** contiguity of the malar stripe with the hood, **(C)** malar stripe prominence and **(D)** malar stripe length in web-sourced photographs of peregrine falcons. Elongation scores were calculated by dividing the length score by the width score for each observation.

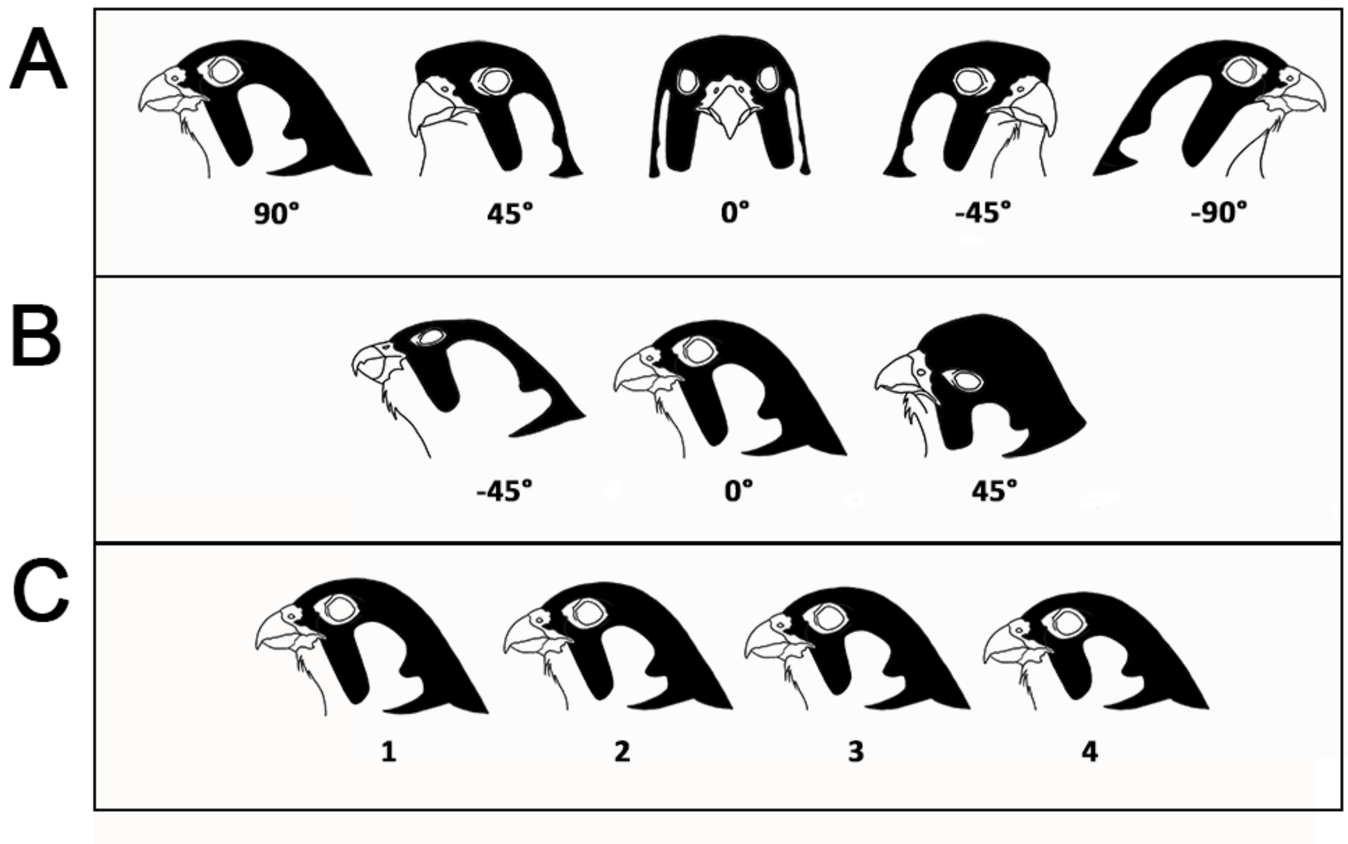

Figure S3. Diagram illustrating the visual scales used to quantify and score **(A)** horizontal head angle, **(B)** vertical head angle, and **(C)** vertical head compression or degree of shoulder hunching in web-sourced photographs of peregrine falcons.

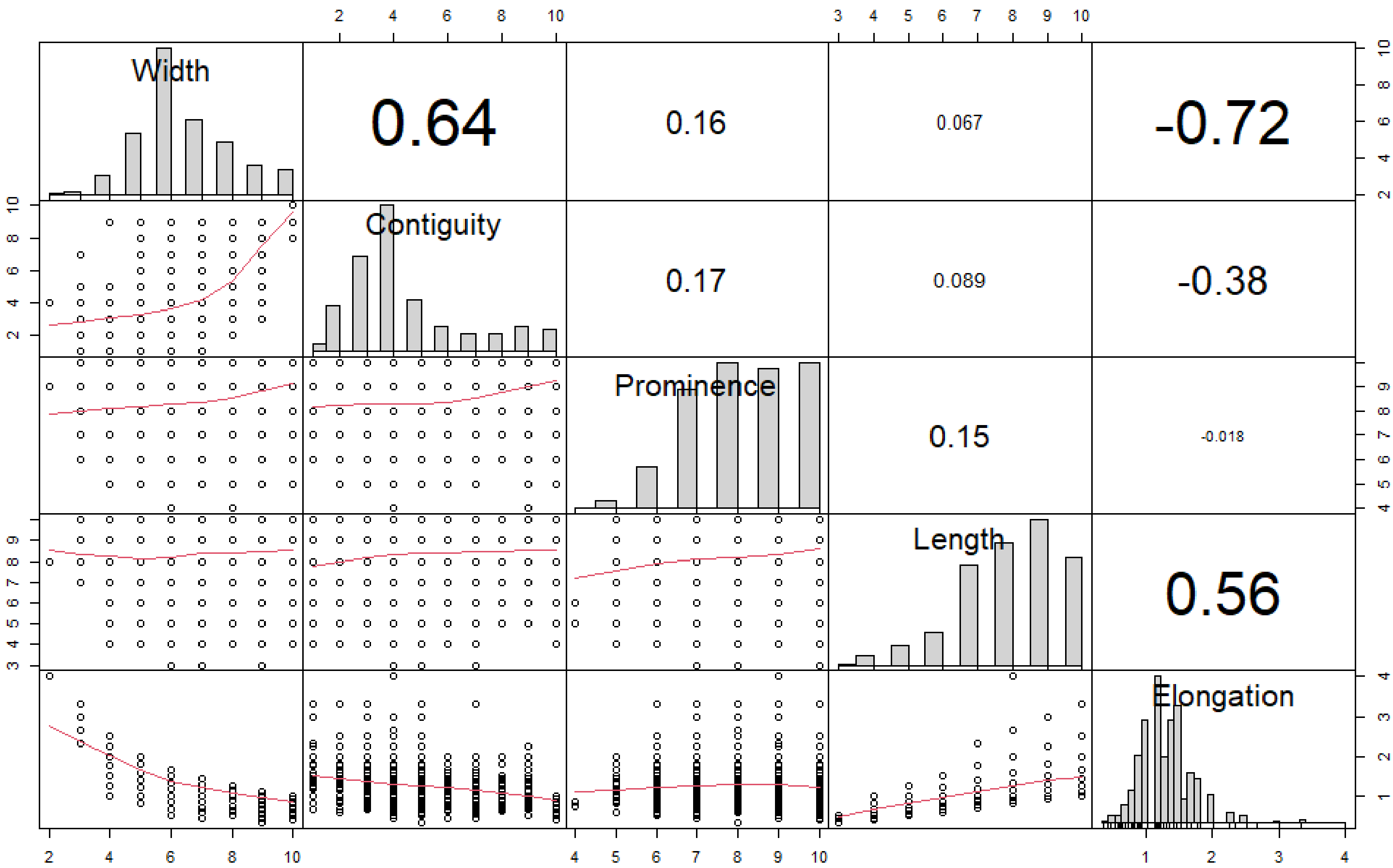

Figure S4. Correlation matrix showing the distributions of the five malar stripe variables and correlations between them. This plot was constructed using the R package PerformanceAnalytics [5].

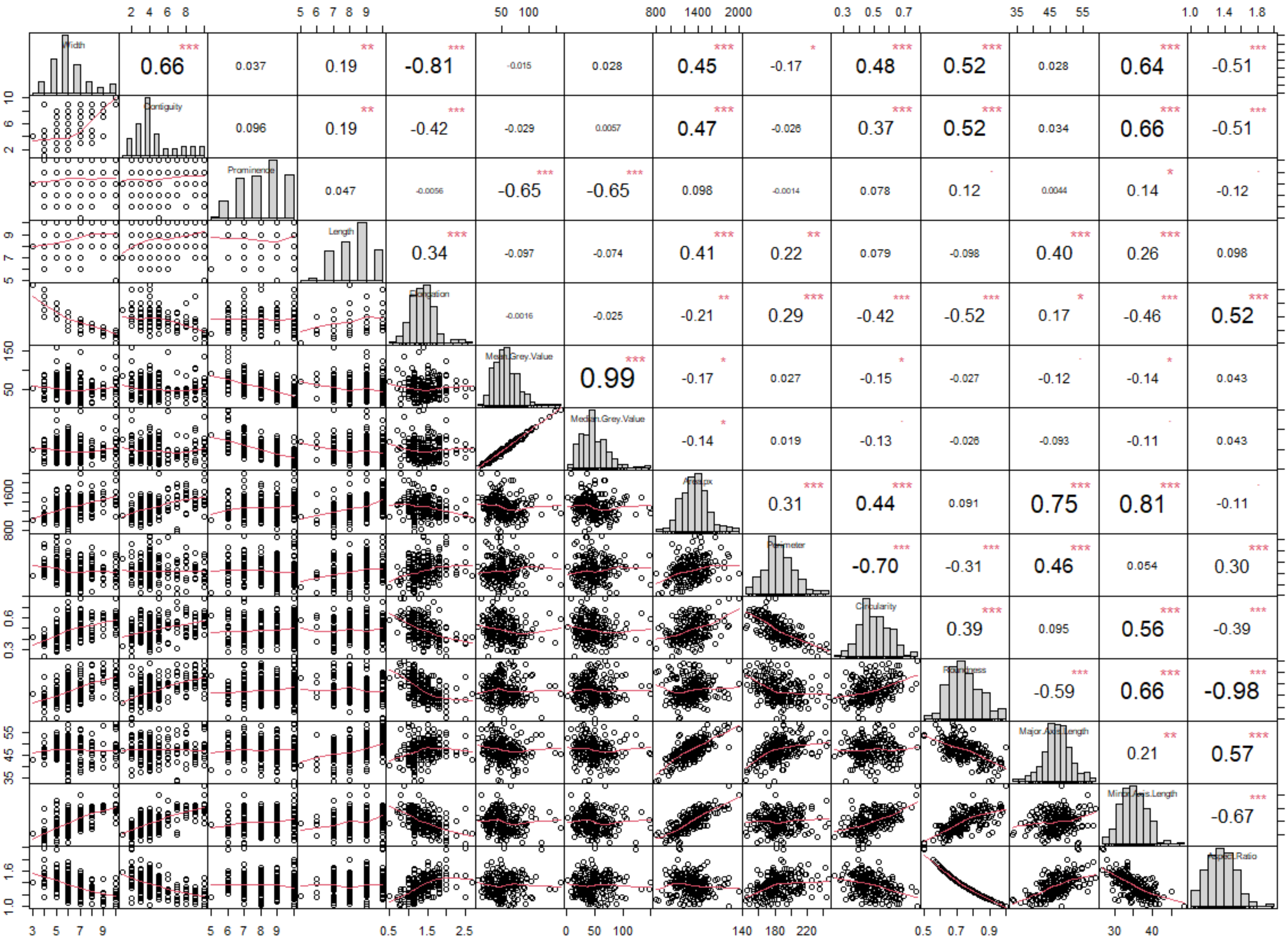

Figure S5. Correlation matrix showing the distributions of the quantitative and subjective measurements of malar stripe characteristics in a subset of the peregrine dataset (N = 213), and correlations between them. (In order from top to bottom and from left to right: width (score), contiguity with the hood (score), prominence (score), length (score), elongation (length score/width score), mean pixel grey value, median pixel grey value, area (px), perimeter (px), circularity, roundness, major axis length (px), minor axis length (px), and aspect ratio (major axis length/minor axis length)). Asterisks represent significance levels for the Pearson's product-moment correlation test: . = p < 0.1, * = p < 0.05, ** = p < 0.01, *** = p < 0.001. This plot was constructed using the R package PerformanceAnalytics [5].

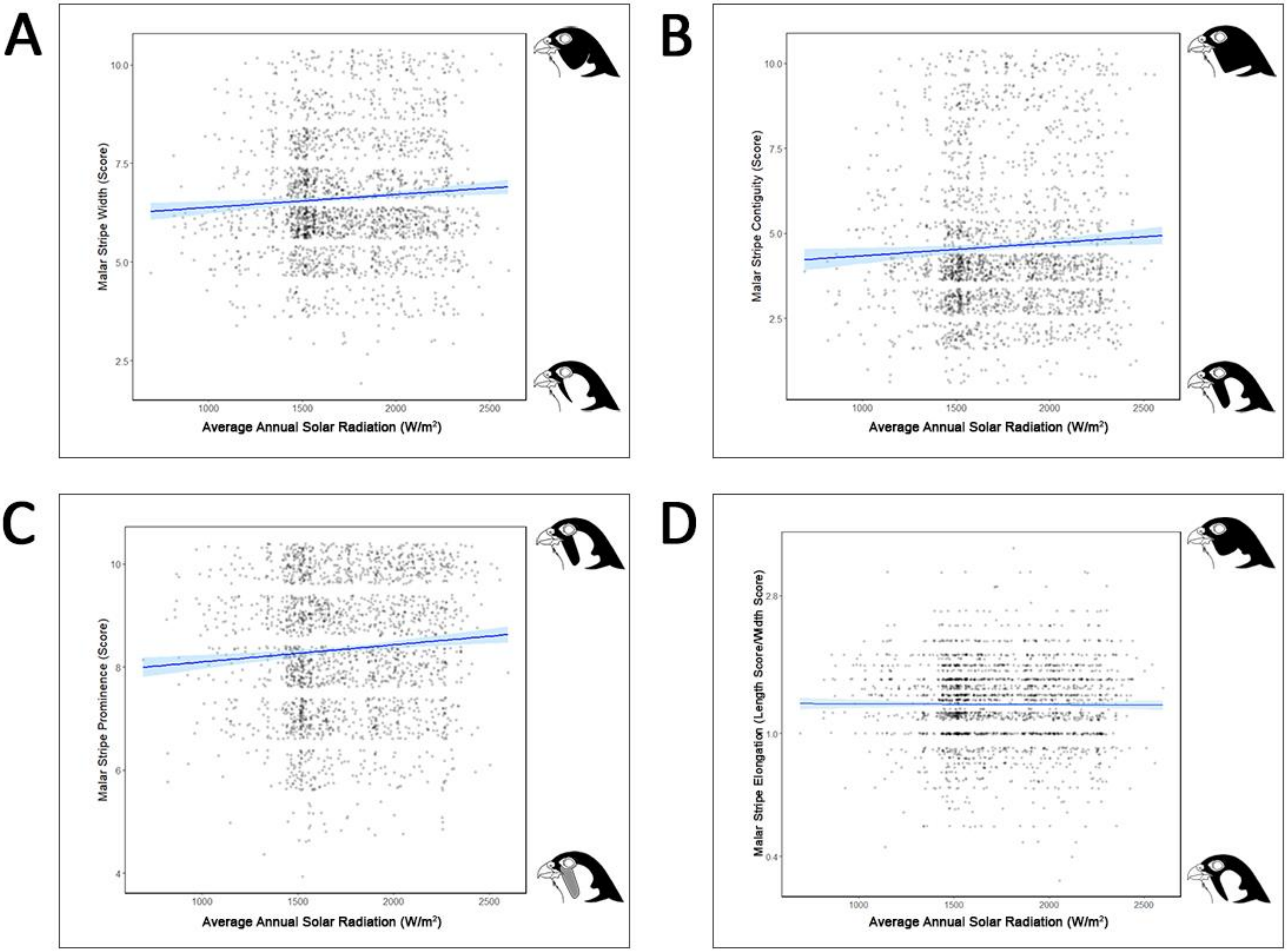

Figure S6. Relationships between average annual solar radiation (W/m^2) and **(A)** malar stripe width, **(B)** contiguity of the malar stripe with the hood, **(C)** malar stripe prominence and **(D)** malar stripe elongation (length/width). Shaded bands represent 95% confidence intervals. Datapoints are shown with 20% jitter to aid in visual interpretation. Elongation scores are shown on a log scale to aid visual interpretation, due to the presence of outliers in the data. Plots were constructed using the R package ggplot2 [6].

Supplementary References

[1] Ferguson-Lees, J. and Christie, D. A. 2001. Raptors of the world. – A&C Black.

[2] Wink, M. 2018. Phylogeny of Falconidae and phylogeography of Peregrine Falcons. – Ornis Hungarica 26(2): 27–37.

[3] Schneider, C. A., Rasband, W. S. and Eliceiri, K. W. 2012. NIH Image to ImageJ: 25 years of image analysis. – Nat. Methods 9(7): 671-675. PMID: 22930834.

[4] Ferreira, T. and Rasband, W. S. 2012. ImageJ User Guide (IJ 1.46r Revised Edition). - National Institutes of Health, USA, https://imagej.nih.gov/ij.

[5] Peterson, B.G., Carl, P., Boudt, K., Bennett, R., Ulrich, J. and Zivot, E. 2014. PerformanceAnalytics: Econometric tools for performance and risk analysis. R package version 1(3541): 107.

[6] Wickham, H. 2016. ggplot2: Elegant Graphics for Data Analysis. – Springer-Verlag.

[7] Vrettos, M., Reynolds, C. and Amar, A. 2021. Data from: Malar stripe size and prominence in peregrine falcons vary positively with solar radiation: support for the solar glare hypothesis. – Dryad Digital Repository. https://doi.org/10.5061/dryad.b8gtht7c9.